

Supervised Reward Inference

Will Schwarzer^{*1}, Jordan Schneider^{†2}, Philip S. Thomas¹, and Scott Niekum¹

¹University of Massachusetts

²Anthropic

Abstract

Existing approaches to reward inference from behavior typically assume that humans provide demonstrations according to specific models of behavior. However, humans often indicate their goals through a wide range of behaviors, from actions that are suboptimal due to poor planning or execution to behaviors which are intended to communicate goals rather than achieve them. We propose that supervised learning offers a unified framework to infer reward functions from any class of behavior, and show that such an approach is asymptotically Bayes-optimal under mild assumptions. Experiments on simulated robotic manipulation tasks show that our method can efficiently infer rewards from a wide variety of arbitrarily suboptimal demonstrations.

1 Introduction

In order for artificial agents to achieve human goals, humans must first communicate their goals to the agents. While the traditional method of goal communication in reinforcement learning (RL) is explicit reward specification, specifying correct rewards can be challenging [1, 2, 3, 4]. This has highlighted the need for alternative modalities for reward specification, such as human demonstrations, the modality studied in inverse reinforcement learning (IRL) [5].

IRL generally assumes that demonstrations are generated according to a specific model of human behavior, which ranges from noisy optimality [5, 6, 7, 8, 9, 10] to bounded reasoning [11, 12, 13] and beyond. Yet while such models produce solvable learning problems, they are still far from accurate descriptions of the entirety of human behavior. First, real-world human behavior demonstrates all of these suboptimality at once, and many more that have yet to be accounted for [14, 15]; second, people frequently use entirely non-optimal behavior such as gestures in order to communicate their goals.

In this paper, we investigate one approach to learning rewards from the full range of human behavior: framing a human’s actions as an *indication* of their goals, rather than an attempted *optimization* of them. Similar to previous work [16, 17, 15], we assume access to a dataset of behaviors (e.g., demonstrations or gestures) and their associated ground-truth rewards. However, rather than explicitly learning a behavior model that maps these rewards onto the behaviors, we use supervised learning to directly learn a mapping of behaviors onto rewards. This approach, which we call Supervised Reward Inference (SRI), is fast, data efficient, and asymptotically Bayes-optimal (see Sections 5 and 6).

2 Related Work

To the best of our knowledge, our work is the first study of reward inference from general behavior. Here, we review prior work extending behavior imitation [19] and reward inference [5] to use training data, account for various kinds of suboptimality, and learn from behavior classes other than demonstrations.

Meta-IRL Prior work has studied the use of multi-task demonstration datasets to improve the efficiency of IRL inference, under the names of multi-task IRL [20, 21, 22, 23], meta-IRL [24, 25, 26, 27], and lifelong IRL [28]. Similarly to SRI, such works allow fast, data-efficient reward inference, but do not directly enable reward inference from suboptimal demonstrations.

Behavior model misspecification Armstrong and Minderhann [29] showed that it is generally impossible to simultaneously infer a demonstrator’s reward function and their behavior model; thus, reward inference methods must either assume the behavior model (as most methods do) or learn it from data (as Shah et al. [15] and SRI do). Later, Skalse and Abate [30] showed theoretically that assuming behavior models is dangerous, as it almost always produces incorrect reward functions when the model is incorrect. For example, assuming Boltzmann rationality will only provide an asymptotically correct optimal policy set for ground-truth behavior models that take optimal actions most frequently, and no oth-

^{*}Correspondence to: wschwarzer@umass.edu

[†]Work done while at the University of Texas.

Table 1: Comparison of several reward inference methods. Inverse planning refers to Algorithm 1 by Shah et al. [15]. The final three capabilities refer to the ability to infer at least Bayes-optimal rewards from demonstrations generated according to the specified type of behavior; for the latter two types, this assumes access to a dataset of demonstrations drawn from the same distribution (including the same behavior model) as the inference demonstrations. For CIRL [18], we assume a non-interactive CIRL game with one demonstration and one deployment phase. Extensions of Algorithm 1 by Shah et al. [15] may be able to infer correct rewards from arbitrarily suboptimal behaviors in the settings we consider, and possibly from a small number of observed trajectories, but the current algorithm cannot (see Section 2).

Capability	IRL	Meta IRL	CIRL	Inverse Planning	SRI
No reward dataset required	✓	✓	✓	✗	✗
Few-shot inference	✗	✓	✗	✗	✓
Simulator-free reward inference	✗	✓	✗	✓	✓
LfO possible	✓	✓	✓	✗	✓
Known suboptimal behavior class	✓	✓	✓	✓	✓
Limited suboptimal behavior class	✗	✗	✗	✓	✓
Arbitrary behavior class	✗	✗	✗	✗	✓

ers. Other works quantified the error induced by incorrect behavior models: Shah et al. [15] and Chan et al. [8] showed that a variety of misspecifications can induce sometimes dramatically incorrect reward functions, while Hong et al. [31] showed that in continuous-action MDPs, even arbitrarily small errors in the behavior model can result in almost arbitrarily large errors in the inferred reward parameters.

Learning from suboptimal demonstrations Reward inference algorithms have been developed to account for a wide variety of specific suboptimalities in human behavior, including hyperbolic discounting, myopia, false beliefs and bounded cognition [11, 12, 13], autocorrelated action noise [7], mistaken transition models [17], and risk-sensitive behavior [32, 33]. Notably, humans have little trouble inferring and accounting for each other’s suboptimality [12, 13].

Shiarlis et al. [34] studied the setting where demonstrations are arbitrarily suboptimal, but they are labeled as failures (to be avoided) or successes; similarly, Brown et al. [35] used preferences over suboptimal demonstrations. Brown et al. [36] and Chen et al. [37] augment that paper by using noise injection to automatically rank synthetic demonstrations, learning a reward model that dispreers noisy trajectories.

Learning from general behavior Hadfield-Menell et al. [18] and Malik et al. [38] studied how to provide and learn from demonstrations which are selected according to their information content for the other agent, rather than how much reward they accumulate. Shah et al. [15] developed the research direction which is closest to SRI. They present two algorithms for human behavior models and rewards, both based on value iteration networks (VINs) [39], and differentiable planners in general. While the second algorithm they present uses a heuristic to infer rewards from near-optimal agents, the first algorithm uses a similar setting to SRI: it trains a value iteration network on a dataset of demonstration policies and corresponding reward functions to predict a policy given a reward function. Then, at inference time, given a policy, the reward function is recovered through gradient descent. Unlike

SRI, however, this algorithm expects the demonstrator’s full policy at inference time, and has not been extended to continuous domains (which are beyond the default capabilities of VINs).

3 Background

While SRI does not assume that human behavior is generated by any particular learning or control algorithm, we still formalize the notions of “behavior” and “goals” using notation from reinforcement learning (RL) [40] and inverse reinforcement learning (IRL) [5], which we review here.

Control problems studied in RL are formalized mathematically as a Markov decision process (MDP). An MDP $\mathcal{M} = (\mathcal{S}, \mathcal{A}, p, r, d_0, \gamma)$ consists of possibly infinite sets of states, \mathcal{S} , and actions, \mathcal{A} ; a transition function $p : \mathcal{S} \times \mathcal{A} \times \mathcal{S} \rightarrow [0, 1]$; a reward function $r : \mathcal{S} \times \mathcal{A} \rightarrow \mathbb{R}$; an initial state distribution $d_0 : \mathcal{S} \rightarrow [0, 1]$; and a discount factor $\gamma \in [0, 1]$.

A policy $\pi : \mathcal{S} \times \mathcal{A} \rightarrow [0, 1]$ is a function describing the agent’s probability of selecting an action in any given state; let Π be the set of all policies. Policies interact with an MDP to produce stochastic processes known as episodes: $(S_0, A_0, R_0, S_1, A_1, R_1, \dots)$ such that $S_0 \sim d_0$, $A_t \sim \pi(S_t, \cdot)$, $R_t = r(S_t, A_t)$, and $S_{t+1} \sim p(S_t, A_t, \cdot)$. MDPs can also be partially observable, meaning they also have a set of observations \mathcal{O} and an emission function $\Omega : \mathcal{S} \times \mathcal{O} \rightarrow [0, 1]$. In this case, episodes include observations generated by the emission function, $O_i \sim \Omega(S_i, \cdot)$, and the policy $\pi : \mathcal{O} \times \mathcal{A} \rightarrow [0, 1]$ instead maps observations to actions: $A_i \sim \pi(O_i, \cdot)$.

In the notation used in this paper, we assume for simplicity that the reward function can be described as a function of state alone: $(R_t \perp\!\!\!\perp A_t | S_t)$. Thus, we will write $r(S_t)$ for brevity. Such state-based rewards are common in goal-based robotic manipulation tasks, for example. However, our methods apply equally well to the case where actions influence the reward.

The objective of an RL agent in an MDP is to accumulate as much reward as possible, subject to exponential time discounting. Formally, the discounted return starting at time t is the sum of rewards at and after t , discounted exponentially by γ : $G_t = \sum_{i=0}^{\infty} \gamma^i R_{t+i}$. The expected discounted episodic return in an MDP is the expected value of G_0 for a given policy: $J(\pi) = \mathbb{E}[G_0; \pi]$, where semicolon π indicates that $A_t \sim \pi(S_t, \cdot)$. RL in a given MDP is thus the optimization problem $\arg \max_{\pi} J(\pi)$. Let π^* be such an optimal policy, and let its expected return be J^* .

Reward Inference. In reward inference problems such as SRI, IRL, or CIRL, the reward function is unknown to the agent, but typically train-time access to the underlying reward-free MDP, $\mathcal{M} \setminus \{r\}$, is still assumed.¹ In place of the reward, some number of trajectories in the environment are provided, consisting of sequences of either observations, states, or states and actions.² In settings where the human behaves roughly optimally for the task they intend the imitator to complete, these trajectories are called *demonstrations*, but for generality we call them “behavior trajectories”. In this paper, we will assume the most difficult setting, where trajectories are sequences of observations: $\tau = (o_0, o_1, \dots, o_{L_B}) \in \mathcal{T}$, where $\mathcal{T} := (\mathcal{O})^{L_B}$. Thus, to indicate a single task, the agent is provided with $\{\tau_n\}_{n=1}^N \in \mathcal{T}^N$.

The agent’s goal is to use these trajectories to infer the reward function. The reward function itself is sometimes the final output, but our focus is on optimizing the inferred reward function and evaluating the resulting policy against the hidden ground truth reward function.

3.1 Learning Behavior Models from Known Rewards

Reward inference models traditionally infer a completely unknown reward function r by assuming that the trajectories $\{\tau_n\}$ are generated according to a specific, known mapping $b : \mathcal{R} \rightarrow \Pi$, where \mathcal{R} is the space of reward functions [6, 30]. However, some recent work has partially inverted this setting, instead assuming that the *behavior model* is partially or completely unknown, but can be inferred from samples of human behavior collected for partially or completely known *reward functions*. For example, Reddy et al. [17], Enayati et al. [16], Carreno-Medrano et al. [41], and Ghosal et al. [42] use demonstrations by humans in tasks with known rewards to infer parameters of their behavior models, such as their Boltzmann-rationality temperature parameter or their internal beliefs about the transition model, p ; similarly, Milliken and Hollinger [43] estimate a human’s expertise in a driving task using the knowledge that hitting obstacles is undesirable. Finally, in their first algorithm, Shah et al. [15] use a dataset of known reward functions and known policies to learn any behavior model that can be produced by a value iteration network

¹In this paper, we use “reward inference” to denote reward inference from behavior, such as IRL.

²This setup describes a two-phase CIRL game; CIRL allows for multiple learning-deployment interactions between agent and demonstrator, but such an interactive problem setup is beyond the scope of this paper.

in a tabular MDP.

4 Supervised Reward Inference

In our work, we study a simpler approach for performing reward inference using a dataset of human behavior for known rewards. Rather than training a parameterized behavior model from data, we simply train the inverse model to directly map trajectories to reward functions.

This direct reward function inference approach, if it performed N -shot inference (i.e., used N trajectories as input) with trajectories of length L_B , would produce a model from trajectories to reward functions $f_{\theta} : \mathcal{T}^N \rightarrow \mathcal{R}$, allowing reward inference on a single state s through $f_{\theta}(\{\tau_n\}_{n=1}^N)(s)$. Such a model would work well in those cases studied previously where the exact reward function is known [15], or where a parameterized form r_{ψ} of the reward function is known, in which case f_{θ} could use ψ as its target. However, this is not a general solution, as true human reward functions in complex environments are unlikely to have known parameterizations (see Section 4.2).

Instead, we teach f_{θ} to predict samples of the reward given a state as input: $r(s) \approx f_{\theta}(\{\tau_n\}_{n=1}^N, s)$. A further enhancement offers an immense efficiency gain: the behavior trajectories (and thus task) need not be reprocessed at every timestep, and can instead be preprocessed into a task encoding. We call the resulting task encoder f_{θ_f} (the **blue path** in Figure 1), and the state-encoder and final reward model g_{θ_g} (the **red path** in Figure 1).³ This final structure allows us to formally define SRI.

Definition 4.1 (Supervised Reward Inference). Given: **a**) a random set of behavior trajectories $\{T_n\}_{n=1}^N \in \mathcal{T}^N$ and a random reward function R jointly following a distribution \mathcal{D}_T ; **b**) a random state S following some distribution \mathcal{D}_S ; **c**) some parameterized function families $f_{\theta_f} : \mathcal{T}^N \rightarrow \Psi$ and $g_{\theta_g} : S \times \Psi \rightarrow \mathbb{R}$; and **d**) some regression loss function $\mathcal{L} : \mathbb{R} \times \mathbb{R} \rightarrow \mathbb{R}$, *supervised reward inference* (SRI) is the following minimization problem:

$$\arg \min_{\theta_f, \theta_g} \mathbb{E} \left[\mathcal{L} \left(g_{\theta_g}(S, f_{\theta_f}(\{T_n\}_{n=1}^N)), R(S) \right) \right].$$

See Algorithm 1 for an example gradient-descent-based implementation. Note that the state samples that are labeled with rewards do **not** need to be taken from the behavior trajectories. Indeed, it is often best for states and behaviors to be separate: the state samples should be representative of the state space optimized during RL, but the behaviors need not be.

4.1 Example Architecture

Figure 1 demonstrates the abstract structure of the architecture that we used for SRI in our experiments; see Appendix B for

³Note that this structure also allows us to train multi-task policies by conditioning on the task embedding output from f_{θ_f} [25], which we explore in experiments with reach tasks.

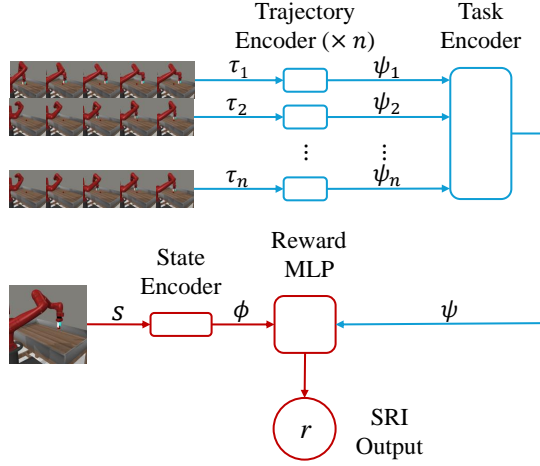


Figure 1: Example SRI model architecture. Behavior trajectories are processed independently into trajectory representations by a sequence model such as a transformer, and then these representations are combined into an overall task representation ψ by a set model such as a set transformer [44] (blue path). This computation is done only *once per task*. Independently, the current state is processed into a representation ϕ by a standard multi-layer perceptron or convolutional neural network (red path). This process is done *once per timestep*, but is very fast: it consists of one forward pass through two small MLPs. Finally, the task and observation representations are combined by another multi-layer perceptron into a scalar reward.

exact details. All g_{θ_g} networks used (red path) were MLPs, while the trajectory encoder was a transformer [45], and the task encoder was a set transformer [44].

4.2 Dataset Construction

As discussed in Section 3.1, prior work suggests one straightforward way of constructing a behavior-reward dataset for SRI: collect human behavior attempting to optimize known reward functions. Because the reward functions are known, states can be arbitrarily sampled (following whatever \mathcal{D}_S is desired) and labeled computationally. Such an approach offers a limited number of behavior samples but an arbitrary number of state-reward pairs, which our experiments suggest is sufficient for strong performance (see Tables 3 and 4 in Section 6). Our experiments follow this approach, using simulations of suboptimal human behavior.

However, assuming computational access to a ground-truth reward function is not reasonable for most complex environments and tasks, such as those where human goals are implicit rather than explicit or where tradeoffs must be made. In these cases, it may be more feasible to observe human behavior “in the wild” and use human labeling of goals, rewards or preferences, or other computational reward estimation methods, such as reward inference from their speech or facial expressions [46]. In such a scenario, state-reward samples could be

Algorithm 1 SRI Training with Gradient Descent

1: **Input:** Number of training tasks K , number of trajectories per task N_T , number of state-reward samples per task N_s , batch size M , number of inference trajectories per task N_I , learning rate α , and training dataset

$$\mathcal{D} = \left\{ \left(\left\{ \tau_{k,n} \right\}_{n=1}^{N_T}, \left\{ (s_{k,n}, r_{k,n}) \right\}_{n=1}^{N_s} \right) \right\}_{k=1}^K$$

2: Initialize $f_{\theta_f} : \mathcal{T}^{N_I} \rightarrow \mathbb{R}^d$

3: Initialize $g_{\theta_g} : \mathcal{S} \times \mathbb{R}^d \rightarrow \mathbb{R}$

4: **repeat**

5: Sample batch of behavior and state-reward samples,

$$\left\{ \left(\left\{ \tau_{k,n} \right\}_{n=1}^{N_T}, \left\{ (s_{k,n}, r_{k,n}) \right\}_{n=1}^{N_s} \right) \right\}_{k=1}^M \sim \mathcal{D}$$

6: Randomly sample N_I trajectories from each set of N_T

$$(\psi_{k,n})_{k=1,n=1}^{M,N_s} = \left(f_{\theta_f} \left(\left\{ \tau_{k,n} \right\}_{n=1}^{N_I} \right) \right)_{k=1,n=1}^M$$

$$(\hat{r}_{k,n})_{k=1,n=1}^{M,N_s} = \left(g_{\theta_g} (s_{k,n}, \psi_{k,n}) \right)_{k=1,n=1}^{M,N_s}$$

$$9: \mathcal{L}(\theta_f, \theta_g) \leftarrow \frac{1}{MN_s} \sum_{k=1}^M \sum_{n=1}^{N_s} (\hat{r}_{k,n} - r_{k,n})^2$$

$$10: \theta_f \leftarrow \theta_f - \alpha \nabla_{\theta_f} \mathcal{L}(\theta_f, \theta_g)$$

$$11: \theta_g \leftarrow \theta_g - \alpha \nabla_{\theta_g} \mathcal{L}(\theta_f, \theta_g)$$

12: **until** convergence

13: **Output:** Learned demonstration encoder f_{θ_f} and reward model g_{θ_g}

taken from the observed behavior itself, though care will have to be taken to ensure their representativeness of the RL state space.

5 Bayes Optimality of SRI

Are there any classes of behavior which are too suboptimal or arbitrary even for SRI? For which classes of reward inference problems will SRI produce an optimal reward model? In this section, we state the theoretical answer to these questions: as you give it more data, SRI approaches Bayes optimality for *any* reward inference problem as long as the problem and SRI’s model family satisfy certain compactness and ‘niceness’ assumptions. Concretely, in Appendix A, using the Bayesian inverse reinforcement learning framework [6], we formally state and prove the following theorem.

Main Theorem, Paraphrased (Asymptotic Optimality of SRI Algorithms). *Consider an SRI problem in an MDP with jointly distributed reward R and trajectory samples $\{T_n\}_{n=1}^N$. Suppose that the dataset, SRI algorithm, and MDP satisfy the following assumptions.*

Assumptions: 1) The MDP has compact state and action spaces \mathcal{S} and \mathcal{A} and bounded returns; 2) The MDP has a random (unknown) continuous reward function R ; 3) SRI’s model family is $\{f_{\theta}\}_{\theta \in \Theta}$ for compact Θ ; 4) $\{f_{\theta}\}$ is equicontinuous; 5) SRI minimizes mean-squared error, and $\{f_{\theta}\}$ contains the minimizer of mean-squared error, $\mathbb{E}[R | \{T_n\} = \{\tau_n\}]$; 6) We sample trajectories and rewards from the true distribution, and we sample states from a distribution with full support over the state space.

Claim: *As the size of the dataset increases, any SRI algorithm in this setting is asymptotically Bayes-optimal in two senses: first, its inferred reward functions almost surely con-*

verge uniformly over the state space to the expectation of the posterior distribution of R given $\{T_n\}$; second, consequently, the returns of its optimal policies converge almost surely to the maximum expected return under this posterior distribution.

Proof sketch. The proof follows three steps: **1)** show that SRI’s inferred reward function almost surely converges uniformly over the state space to the expectation of the posterior reward; **2)** show that maximizing return under the expectation of the posterior reward is equivalent to maximizing expected return under the posterior; **3)** show that SRI’s uniform convergence in reward accuracy causes its optimal policies to also converge to optimal performance. (Note that all convergence discussed here is almost sure.)

1) To show uniform convergence of SRI’s inferred reward functions over the state space, we first show pointwise convergence. First, boundedness of the reward function and the function family lets us conclude that the loss function is Glivenko-Cantelli, and so converges uniformly over parameters. Thus, any convergent subsequence of our sequence of parameters converges to an optimal θ , and so our sequence of parameters must also converge to an optimal θ .

Next, to conclude uniform convergence of SRI’s reward functions over the state space, we use the assumption of equicontinuity of $\{f_\theta\}$ to apply the Arzelà-Ascoli theorem, which establishes that any convergent sequence of parameters has a subsequence that is uniformly convergent over the state space. The desired result then follows by iterated application of Arzelà-Ascoli on any non-uniformly-convergent subsequence in our sequence of parameters. We therefore conclude that SRI’s inferred reward functions converge uniformly over the state space to the expectation of the posterior reward function.

2) To show that SRI’s limit is the correct maximization target for imitation policies, we generalize a tabular result by Ramachandran and Amir [6]. Concretely, we use Fubini’s Theorem and the Bounded Convergence Theorem to prove that maximizing expected return under the reward posterior is equivalent to maximizing return under the expectation of the reward posterior.

3) Finally, because the MDP’s returns are bounded, and because we can uniformly bound SRI’s deviation from the expected reward posterior across all states, we can also bound the deviation of SRI’s predicted *returns* across all policies. As the quantity of data increases, this return deviation decreases. Therefore, SRI’s optimal policies approach optimality with respect to the expectation of the reward posterior, and hence expected optimality with respect to the reward posterior. \square

6 Experiments

In the previous section, we showed that, theoretically, an ideal SRI algorithm can ideally solve any reward inference task as well as it is possible to solve it. In this section, we demonstrate this ability in practice, using several concrete examples of

tasks that are not possible to solve with previous methods: inferring a pick-place reward function from a gesture, inferring correct goals from demonstrations that systematically show the *wrong* goal, and more.

However, in addition to providing evidence that SRI can infer reward functions from radically suboptimal demonstrations, as expected, we also designed experiments to explore the following concrete questions about SRI’s behavior: **1)** Can SRI learn models that infer sharp complex, discontinuous reward functions precisely? **2)** Can SRI learn models that infer reward functions from behaviors like gestures that each indicate the goal only indirectly or partially? **3)** How does the performance of SRI models relative to classical imitation learning models change as the suboptimality of the demonstrations increases? **4)** How does the performance of SRI models vary with respect to amount of training data and number of test-time demonstrations?

6.1 Experiment Design

For additional experimental details, see Appendix C.

Tasks. Ground-truth tasks are Meta-World pick-place and reach tasks [47] with randomly distributed goals. Because we do not use the ground-truth reward function to evaluate policies, we added an additional discontinuous reward of 5.0 upon success in order to test SRI’s ability to infer sharp reward functions.

Demonstrations. Experiments used five classes of behavior trajectories, all generated by oracular policies with reach goals. **Gestures (GESTURE):** robot hand starts at a random position above the table and reaches towards the goal for 50 timesteps. Used for pick-place tasks. **Noisy actions (NOISY $_\epsilon$):** the hand starts in the default location and reaches directly towards the goal for 150 timesteps, but with a probability ϵ each timestep of instead reaching towards a random location. Noisy actions with random starts (**NOISY GESTURE $_\epsilon$**): uses random actions like NOISY $_\epsilon$, but otherwise identical to GESTURE (including a horizon of 50). **Goal offset (PSYCHIC $_\alpha$):** the hand reaches deterministically towards the *wrong* position, offset towards the origin by some amount ($\alpha = 1.0$ is no offset, while -1.0 is mirroring through the origin). Finally, mirrored and circled (**HARD**): the hand starts at the origin, then draws a circle around a deterministically incorrect position.

Except where otherwise specified, we provided 100 demonstrations per task for GESTURE, NOISY, and NOISY GESTURE, 1 demonstration for the deterministic PSYCHIC, and 10 demonstrations for HARD.

State-reward Sampling. For all tasks, SRI received a state-reward dataset (see Section 4.2) with states produced by the robot hand attempting to reach to random locations on and around the table while randomly opening and closing its gripper. For pick-place tasks, SRI also received examples of states from an oracular pick-place agent bringing the object to random positions. Of course, SRI could not infer goals from such states, as they were randomly shuffled and uncorrelated with the goal of the task it was attempting to infer.

Table 2: Performance of SRI and baselines on pick-place tasks given demonstrations from the GESTURE class (see Section 6.1). Performance is measured by the object’s average proximity to the goal under each method’s learned policy, clipped per-trial to a minimum of 0 (see Section 6.1), with standard error variance over 30 trials. Results show that SRI can infer a complex reward function from completely non-optimal gestures as demonstrations.

<i>Method</i>	<i>Ave. Goal Proximity</i>
SRI	0.822 ± 0.051
GAIL	-0.001 ± 0.000
AIRL	-0.001 ± 0.001
BC	-0.001 ± 0.000
GT RL	0.903 ± 0.011

Data quantity. Except where otherwise noted, SRI received 1,280 tasks, each with 100 demonstrations and 10,000 state-reward pairs (note, however, that such a large amount of data was unnecessary; see Tables 3 and 4). For pick-place tasks, 80% of states were from random reaching, while 20% were from random pick-placing.

RL. For learning policies with SRI’s learned reward functions, we used Truncated Quantile Critics [48] for reach tasks and Proximal Policy Optimization [49] for pick-place tasks, each as implemented in Stable-Baselines3 [50].

For reach tasks, which are easier, we trained multi-task policies by conditioning the policy on the task representation ψ ; for pick-place tasks, we trained task-specific policies (though note that all tasks within each trial were inferred by a single SRI model).

Metrics and statistics. The evaluated metric is average normalized goal proximity: 1 minus the distance to the goal of the hand (for reach tasks) or object (for pick-place tasks), scaled such that the initial distance is 1, and averaged across all timesteps and trials. To avoid distraction by large negative proximity values in plots, we clip average proximity of each trial in plots to a minimum of 0 (but do not clip in tables).

All methods and all settings in all experiments were run for 30 trials, and statistical uncertainty was quantified using standard error without Bonferroni correction.

Baselines. We used four baselines for comparison. First, three imitation learning baselines, for all of which we used the Imitation library in Python [51]: behavioral cloning (BC) [19], generative adversarial imitation learning (GAIL) [52] and adversarial inverse reinforcement learning (AIRL) [53]. Finally, we also used a ground-truth RL baseline (GT RL), consisting of policies learned through RL with the ground-truth reward.

6.2 Results

Throughout our experiments, we discovered that SRI was capable of learning reward functions with a high degree of accuracy (see Table 2), in a wide variety of situations where optimality-

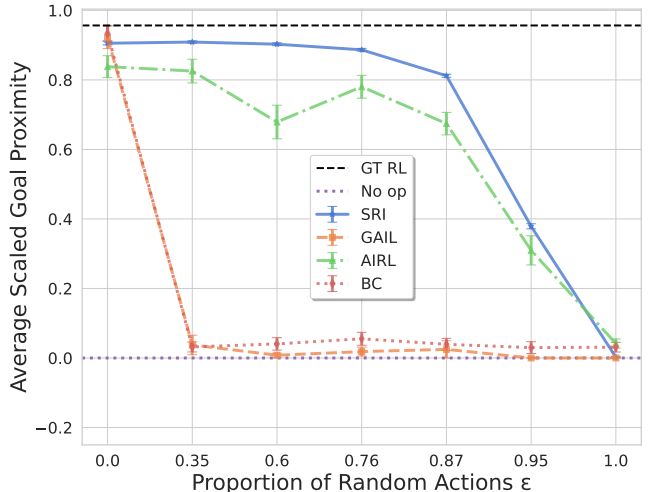


Figure 2: Performance of SRI and baselines when given noisy demonstrations. Error bars indicate standard error over 30 trials. Tasks are Meta-World reach tasks with demonstrations from the NOISY GESTURE $_{\epsilon}$ class for various values of ϵ (see Section 6.1). Performance is measured by the robot hand’s average proximity to the goal under each method’s learned policy, clipped per-trial to a minimum of 0 (see Section 6.1), with 30-trial standard error bars. Note that $\epsilon = 1.0$ is effectively impossible, as demonstrations are pure noise, and is only included for completeness. Results show that SRI approaches ground-truth RL performance in the presence of perfect demonstrations, and suffers less from noisily suboptimal demonstrations than other methods.

Table 3: Performance of SRI trained on varying numbers of tasks and observations per task, with baseline results as follows: GAIL: -1.808 ± 0.368 ; AIRL: -1.582 ± 0.302 ; BC: -0.930 ± 0.083 ; Ground Truth RL: 0.957 ± 0.005 . Variance is measured with 30-trial standard error. Tasks are Meta-World reach tasks with demonstrations from the HARD class (see Section 6.1). Performance is measured by the robot hand’s average proximity to the goal under each method’s learned policy, clipped per-trial to a minimum of 0 (see Section 6.1). Results show that despite the difficulty of reward inference from HARD demonstrations, and despite SRI’s complex deep architecture, SRI needs surprisingly little data to learn reasonable reward functions for this task, making do with as little as 8,000 labeled observations.

<i>Num. Tasks</i>	<i>Number of Labeled Observations per Task</i>		
	100	1000	10000
1280	0.860 ± 0.006	0.916 ± 0.004	0.930 ± 0.003
320	0.780 ± 0.007	0.866 ± 0.006	0.893 ± 0.006
80	0.495 ± 0.017	0.792 ± 0.008	0.812 ± 0.010

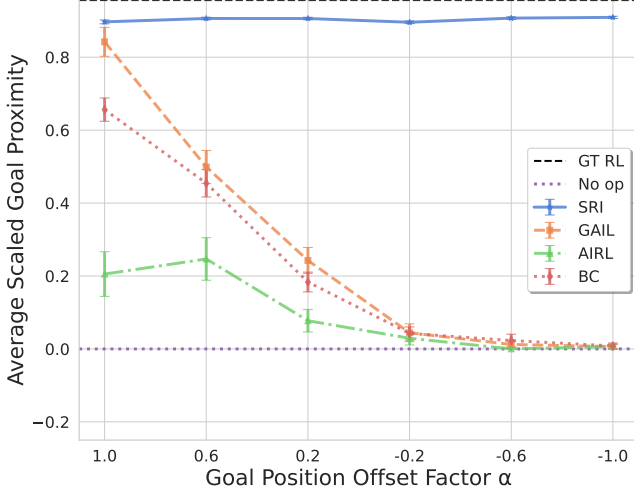


Figure 3: Performance of SRI and baselines when given demonstrations that deterministically reach to the wrong location. Tasks are Meta-World reach tasks with demonstrations from the PSYCHIC $_{\alpha}$ class (see Section 6.1) for various values of α . Performance is measured by the robot hand’s average proximity to the goal under each method’s learned policy, clipped per-trial to a minimum of 0 (see Section 6.1), with 30-trial standard error bars. Results show that the performance of optimality-assuming algorithms decreases to zero with sub-optimality of the demonstrations, while SRI’s learned policies remain nearly optimal regardless of demonstration optimality.

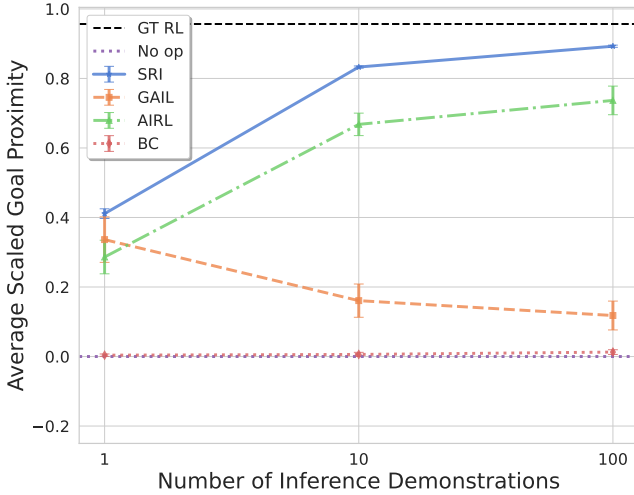


Figure 4: Performance of SRI and baselines when given varying numbers of noisy demonstrations. Tasks are Meta-World reach tasks, with demonstrations from the NOISY $_{0.87}$ class (see Section 6.1). Performance is measured by the robot hand’s average proximity to the goal under each method’s learned policy, clipped per-trial to a minimum of 0 (see Section 6.1), with 30-trial standard error bars. Results show that SRI performs better than optimality-assuming methods regardless of demonstration quantity.

Table 4: Performance of SRI trained on varying numbers of tasks and observations per task, with baseline results as follows: GAIL: -0.004 ± 0.002 ; AIRL: -0.001 ± 0.000 ; BC: -0.002 ± 0.001 ; Ground Truth RL: 0.903 ± 0.011 . Variance is measured with 30-trial standard error. Tasks are Meta-World reach tasks with demonstrations from the HARD class (see Section 6.1). Performance is measured by the robot hand’s average proximity to the goal under each method’s learned policy, clipped per-trial to a minimum of 0 (see Section 6.1). Results show that pick-place is a far more difficult task than reach, unsurprisingly (see Table 3), but SRI can still learn well with 320,000 labeled observations. Note that the counterintuitively strong result of 320 tasks and 1000 observations is due to model capacity: with higher-capacity models, we find that SRI’s performance in this experiment increases monotonically with data quantity.

Num. Tasks	Number of Labeled Observations per Task		
	100	1000	10000
1280	0.614 ± 0.076	0.715 ± 0.069	0.784 ± 0.052
320	0.221 ± 0.067	0.768 ± 0.052	0.708 ± 0.059
80	0.018 ± 0.021	0.269 ± 0.065	0.502 ± 0.085

assuming methods completely fail (Figure 3; Tables 2, 3, 4). It performed well even when the behavior-reward mapping was profoundly noisy (Figure 2), and even when it only received a single noisy demonstration (Figure 4); unsurprisingly, though, it performed even better when the behavior-reward mapping was arbitrarily suboptimal but still invertible (Figure 3). Finally, while challenging reward functions still require a substantial number of labeled observations to be learned accurately (Table 4), potentially necessitating the use of self-supervised learning methods, simpler tasks may be solvable with quantities of data small enough to collect manually (Table 3).

Nevertheless, our results did not come easily: we also discovered that data quality is crucial for SRI’s performance, and that failing to sample states from all regions that a policy might explore can lead SRI to infer a hackable reward function with incorrect local optima. Pick-place tasks were particularly difficult, as the reward model needed to provide accurate pre-grasping shaping rewards in addition to a large, discontinuous success reward; however, limited model capacity often forced the model to reduce error in success prediction, to the detriment of the shaped rewards necessary to find and grasp the object.

In general, reward inference from arbitrary behavior is a fundamentally difficult problem, as the policy and reward function cannot be regularized to be similar to the demonstration. However, one could regularize the policy or reward function to prefer states that are similar to those seen in the state-reward dataset. Future work exploring this direction or iterative data labeling [54] may further reduce the data requirements of SRI.

7 Conclusion

In this paper, we introduced supervised reward inference (SRI), which to our knowledge is the first algorithm to be able to infer accurate reward functions from arbitrary behavior. We showed that SRI is asymptotically Bayesian-optimal, as long as the model is strong enough: as the quantity of training data available to it approaches infinity, its learned policies approach the highest ground-truth return possible given limited behavior at inference time. Finally, we showed that SRI can infer difficult reward functions correctly from behavior with complex suboptimality, and can infer simpler reward functions from suboptimal behavior with only a few thousand labeled states.

Several important questions remain to be answered before SRI can be easily applied to existing real-world problems. First, many real-world tasks will likely be visual, thus requiring an image encoder as part of the SRI model, a change which we believe will be straightforward but did not study here. Second, while SRI’s data efficiency on reach tasks might allow manual dataset construction, real-world tasks are likely to be far more complex than even the simulated pick-place task studied here. In such cases, SRI’s labeled data efficiency may be enhanced through self- and weakly-supervised learning methods. For example, DINOv2 [55] or other visual foundation models could help it learn rewards more easily, while behavior foundation models [56] might help it more easily infer optimal policies.

We believe that SRI’s compatibility with self-supervised foundation models is thus one advantage offering it great promise in the effort to align artificial agents. Just as natural language processing tasks have been made easier through leveraging massive datasets [57], so too we hope that artificial agents can achieve humans’ real-world goals more easily through the power of data.

8 Acknowledgements

We are grateful to Bruno Castro da Silva for his exceptionally generous help in pushing this project to completion. We are also grateful to Russell Coleman for his early work on this project.

This work has taken place in part in the Safe, Correct, and Aligned Learning and Robotics Lab (SCALAR) at The University of Massachusetts Amherst. SCALAR research is supported in part by the NSF (IIS-2323384), the Center for AI Safety (CAIS), and the Long-Term Future Fund. Separately, this work was also supported by the NSF under Grant No. CCF-2018372. Any opinions, findings, and conclusions or recommendations expressed in this material are those of the authors and do not necessarily reflect the views of the National Science Foundation.

References

- [1] Dylan Hadfield-Menell, Smitha Milli, Pieter Abbeel, Stuart J Russell, and Anca Dragan. Inverse reward design. In I. Guyon, U. Von Luxburg, S. Bengio, H. Wallach, R. Fergus, S. Vishwanathan, and R. Garnett, editors, *Advances in Neural Information Processing Systems*, volume 30. Curran Associates, Inc., 2017.
- [2] Ellis Ratner, Dylan Hadfield-Menell, and Anca D. Dragan. Simplifying reward design through divide-and-conquer. In Hadas Kress-Gazit, Siddhartha S. Srinivasa, Tom Howard, and Nikolay Atanasov, editors, *Robotics: Science and Systems XIV, Carnegie Mellon University, Pittsburgh, Pennsylvania, USA, June 26-30, 2018*, 2018. doi: 10.15607/RSS.2018.XIV.048. URL <http://www.roboticsproceedings.org/rss14/p48.html>.
- [3] Serena Booth, W Bradley Knox, Julie Shah, Scott Niekum, Peter Stone, and Alessandro Allievi. The perils of trial-and-error reward design: Misdesign through overfitting and invalid task specifications. In *Proceedings of the 37th AAAI Conference on Artificial Intelligence (AAAI)*, Feb 2023.
- [4] W. Bradley Knox and James MacGlashan. How to specify reinforcement learning objectives. In *Finding the Frame: An RLC Workshop for Examining Conceptual Frameworks*, 2024. URL <https://openreview.net/forum?id=2MGEQNrmDn>.
- [5] A. Y. Ng and S. Russell. Algorithms for inverse reinforcement learning. In *Proceedings of the Seventeenth International Conference on Machine Learning*, 2000.
- [6] Deepak Ramachandran and Eyal Amir. Bayesian inverse reinforcement learning. In *Proceedings of the 20th International Joint Conference on Artificial Intelligence, IJCAI’07*, page 2586–2591, San Francisco, CA, USA, 2007. Morgan Kaufmann Publishers Inc.
- [7] Jiangchuan Zheng, Siyuan Liu, and Lionel M. Ni. Robust bayesian inverse reinforcement learning with sparse behavior noise. *Proceedings of the AAAI Conference on Artificial Intelligence*, 28(1), Jun. 2014. doi: 10.1609/aaai.v28i1.8979. URL <https://ojs.aaai.org/index.php/AAAI/article/view/8979>.
- [8] Lawrence Chan, Andrew Critch, and Anca Dragan. Human irrationality: both bad and good for reward inference, 2021. URL <https://arxiv.org/abs/2111.06956>.
- [9] Cassidy Laidlaw and Anca D. Dragan. The boltzmann policy distribution: Accounting for systematic suboptimality in human models. In *The Tenth International Conference on Learning Representations, ICLR 2022, Virtual Event, April 25-29, 2022*. OpenReview.net,

2022. URL https://openreview.net/forum?id=_l_QjPGN5ye.
- [10] Peter Barnett, Rachel Freedman, Justin Svegliato, and Stuart Russell. Active reward learning from multiple teachers. In Gabriel Pedroza, Xiaowei Huang, Xin Cynthia Chen, Andreas Theodorou, José Hernández-Orallo, Mauricio Castillo-Effen, Richard Mallah, and John A. McDermid, editors, *Proceedings of the Workshop on Artificial Intelligence Safety 2023 (SafeAI 2023) co-located with the Thirty-Seventh AAAI Conference on Artificial Intelligence (AAAI 2023)*, Washington DC, USA, February 13-14, 2023, volume 3381 of *CEUR Workshop Proceedings*. CEUR-WS.org, 2023. URL <https://ceur-ws.org/Vol-3381/48.pdf>.
- [11] Owain Evans, Andreas Stuhlmüller, and Noah D. Goodman. Learning the preferences of bounded agents. In *NIPS Workshop on Bounded Optimality*, 2015.
- [12] Owain Evans, Andreas Stuhlmüller, and Noah D. Goodman. Learning the preferences of ignorant, inconsistent agents. In *Proceedings of the Thirtieth AAAI Conference on Artificial Intelligence*, AAAI’16, page 323–329. AAAI Press, 2016.
- [13] Tan Zhi-Xuan, Jordyn Mann, Tom Silver, Josh Tenenbaum, and Vikash Mansinghka. Online bayesian goal inference for boundedly rational planning agents. In *Proceedings of the 34th International Conference on Neural Information Processing Systems*, pages 19238–19250, December 2020.
- [14] Daniel Kahneman. *Thinking, fast and slow*. Farrar, Straus and Giroux, New York, 2011. ISBN 9780374275631 0374275637.
- [15] Rohin Shah, Noah Gundotra, Pieter Abbeel, and Anca Dragan. On the feasibility of learning, rather than assuming, human biases for reward inference. In Kamalika Chaudhuri and Ruslan Salakhutdinov, editors, *Proceedings of the 36th International Conference on Machine Learning*, volume 97 of *Proceedings of Machine Learning Research*, pages 5670–5679. PMLR, 09–15 Jun 2019. URL <https://proceedings.mlr.press/v97/shahl9a.html>.
- [16] Nima Enayati, Giancarlo Ferrigno, and Elena De Momi. Skill-based human–robot cooperation in tele-operated path tracking. *Autonomous Robots*, 42:997–1009, 2018. URL <https://api.semanticscholar.org/CorpusID:25112243>.
- [17] Siddharth Reddy, Anca D. Dragan, and Sergey Levine. Where do you think you’re going?: Inferring beliefs about dynamics from behavior. In Samy Bengio, Hanna M. Wallach, Hugo Larochelle, Kristen Grauman, Nicolò Cesa-Bianchi, and Roman Garnett, editors, *Advances in Neural Information Processing Systems 31: Annual Conference on Neural Information Processing Systems 2018, NeurIPS 2018, December 3-8, 2018, Montréal, Canada*, pages 1461–1472, 2018.
- [18] Dylan Hadfield-Menell, Anca Dragan, Pieter Abbeel, and Stuart Russell. Cooperative inverse reinforcement learning. In *Proceedings of the 30th International Conference on Neural Information Processing Systems*, NIPS’16, page 3916–3924, Red Hook, NY, USA, 2016. Curran Associates Inc. ISBN 9781510838819.
- [19] Dean A. Pomerleau. Alvin: an autonomous land vehicle in a neural network. In *Proceedings of the 1st International Conference on Neural Information Processing Systems*, NIPS’88, page 305–313, Cambridge, MA, USA, 1988. MIT Press.
- [20] Monica Babeş-Vroman, Vukosi Marivate, Kaushik Subramanian, and Michael Littman. Apprenticeship learning about multiple intentions. In *Proceedings of the 28th International Conference on Machine Learning*, ICML’11, page 897–904, Madison, WI, USA, 2011. Omnipress. ISBN 9781450306195.
- [21] Christos Dimitrakakis and Constantin A. Rothkopf. Bayesian multitask inverse reinforcement learning. In Scott Sanner and Marcus Hutter, editors, *Recent Advances in Reinforcement Learning*, pages 273–284, Berlin, Heidelberg, 2012. Springer Berlin Heidelberg. ISBN 978-3-642-29946-9.
- [22] Jaedeug Choi and Kee-Eung Kim. Nonparametric bayesian inverse reinforcement learning for multiple reward functions. In *Proceedings of the 25th International Conference on Neural Information Processing Systems - Volume 1*, NIPS’12, page 305–313, Red Hook, NY, USA, 2012. Curran Associates Inc.
- [23] Adam Gleave and Oliver Habryka. Multi-task maximum causal entropy inverse reinforcement learning. In *1st Workshop on Goal Specifications for Reinforcement Learning*, FAIM, Stockholm, Sweden, 2018.
- [24] Kelvin Xu, Ellis Ratner, Anca D. Dragan, Sergey Levine, and Chelsea Finn. Learning a prior over intent via meta-inverse reinforcement learning. In Kamalika Chaudhuri and Ruslan Salakhutdinov, editors, *Proceedings of the 36th International Conference on Machine Learning, ICML 2019, 9-15 June 2019, Long Beach, California, USA*, volume 97 of *Proceedings of Machine Learning Research*, pages 6952–6962. PMLR, 2019. URL <http://proceedings.mlr.press/v97/xu19d.html>.
- [25] Lantao Yu, Tianhe Yu, Chelsea Finn, and Stefano Ermon. Meta-inverse reinforcement learning with probabilistic context variables. In H. Wallach, H. Larochelle, A. Beygelzimer, F. d’Alché-Buc, E. Fox, and R. Garnett, editors, *Advances in Neural Information Processing Systems*, volume 32. Curran Associates, Inc., 2019.

- [26] Seyed Kamyar Seyed Ghasemipour, Shixiang (Shane) Gu, and Richard Zemel. Smile: Scalable meta inverse reinforcement learning through context-conditional policies. In H. Wallach, H. Larochelle, A. Beygelzimer, F. d'Alché-Buc, E. Fox, and R. Garnett, editors, *Advances in Neural Information Processing Systems*, volume 32. Curran Associates, Inc., 2019.
- [27] Pin Wang, Hanhan Li, and Ching-Yao Chan. Meta-adversarial inverse reinforcement learning for decision-making tasks. In *2021 IEEE International Conference on Robotics and Automation (ICRA)*, pages 12632–12638, 2021. doi: 10.1109/ICRA48506.2021.9561330.
- [28] Jorge A. Mendez, Shashank Shivkumar, and Eric Eaton. Lifelong inverse reinforcement learning. In *Proceedings of the 32nd International Conference on Neural Information Processing Systems, NIPS'18*, page 4507–4518, Red Hook, NY, USA, 2018. Curran Associates Inc.
- [29] Stuart Armstrong and Sören Mindermann. Occam's razor is insufficient to infer the preferences of irrational agents. In S. Bengio, H. Wallach, H. Larochelle, K. Grauman, N. Cesa-Bianchi, and R. Garnett, editors, *Advances in Neural Information Processing Systems*, volume 31. Curran Associates, Inc., 2018.
- [30] Joar Skalse and Alessandro Abate. Misspecification in inverse reinforcement learning. In *AAAI Conference on Artificial Intelligence*, 2022. URL <https://api.semanticscholar.org/CorpusID:254275448>.
- [31] Joey Hong, Kush Bhatia, and Anca D. Dragan. On the sensitivity of reward inference to misspecified human models. In *The Eleventh International Conference on Learning Representations, ICLR 2023, Kigali, Rwanda, May 1-5, 2023*. OpenReview.net, 2023. URL <https://openreview.net/pdf?id=hJqGbUpDGV>.
- [32] Sumeet Singh, Jonathan Lacotte, Anirudha Majumdar, and Marco Pavone. Risk-sensitive inverse reinforcement learning via semi- and non-parametric methods. *The International Journal of Robotics Research*, 37(13-14):1713–1740, 2018. doi: 10.1177/0278364918772017. URL <https://doi.org/10.1177/0278364918772017>.
- [33] Lillian J. Ratliff and Eric Mazumdar. Inverse risk-sensitive reinforcement learning. *IEEE Transactions on Automatic Control*, 65(3):1256–1263, 2020. doi: 10.1109/TAC.2019.2926674.
- [34] Kyriacos Shiarlis, Joao Messias, and Shimon Whiteson. Inverse reinforcement learning from failure. In *Proceedings of the 2016 International Conference on Autonomous Agents & Multiagent Systems, AAMAS '16*, page 1060–1068, Richland, SC, 2016. International Foundation for Autonomous Agents and Multiagent Systems. ISBN 9781450342391.
- [35] Daniel Brown, Russell Coleman, Ravi Srinivasan, and Scott Niekum. Safe imitation learning via fast Bayesian reward inference from preferences. In Hal Daumé III and Aarti Singh, editors, *Proceedings of the 37th International Conference on Machine Learning*, volume 119 of *Proceedings of Machine Learning Research*, pages 1165–1177. PMLR, 13–18 Jul 2020. URL <https://proceedings.mlr.press/v119/brown20a.html>.
- [36] Daniel S. Brown, Wonjoon Goo, and Scott Niekum. Better-than-demonstrator imitation learning via automatically-ranked demonstrations. In Leslie Pack Kaelbling, Danica Kragic, and Komei Sugiura, editors, *Proceedings of the Conference on Robot Learning*, volume 100 of *Proceedings of Machine Learning Research*, pages 330–359. PMLR, 30 Oct–01 Nov 2020. URL <https://proceedings.mlr.press/v100/brown20a.html>.
- [37] Letian Chen, Rohan Paleja, and Matthew Gombolay. Learning from suboptimal demonstration via self-supervised reward regression. In Jens Kober, Fabio Ramos, and Claire Tomlin, editors, *Proceedings of the 2020 Conference on Robot Learning*, volume 155 of *Proceedings of Machine Learning Research*, pages 1262–1277. PMLR, 16–18 Nov 2021. URL <https://proceedings.mlr.press/v155/chen21b.html>.
- [38] Dhruv Malik, Malayandi Palaniappan, Jaime Fisac, Dylan Hadfield-Menell, Stuart Russell, and Anca Dragan. An efficient, generalized Bellman update for cooperative inverse reinforcement learning. In Jennifer Dy and Andreas Krause, editors, *Proceedings of the 35th International Conference on Machine Learning*, volume 80 of *Proceedings of Machine Learning Research*, pages 3394–3402. PMLR, 10–15 Jul 2018. URL <https://proceedings.mlr.press/v80/malik18a.html>.
- [39] Aviv Tamar, YI WU, Garrett Thomas, Sergey Levine, and Pieter Abbeel. Value iteration networks. In D. Lee, M. Sugiyama, U. Luxburg, I. Guyon, and R. Garnett, editors, *Advances in Neural Information Processing Systems*, volume 29. Curran Associates, Inc., 2016.
- [40] R. S. Sutton and A. G. Barto. *Reinforcement Learning: An Introduction*. MIT Press, Cambridge, MA, 1998.
- [41] Pamela Carreno-Medrano, Abhinav Dahiya, Stephen L. Smith, and Dana Kulić. Incremental estimation of users' expertise level. In *2019 28th IEEE International Conference on Robot and Human Interactive Communication (RO-MAN)*, pages 1–8, 2019. doi: 10.1109/RO-MAN46459.2019.8956320.
- [42] Gaurav R. Ghosal, Matthew Zurek, Daniel S. Brown, and Anca D. Dragan. The effect of modeling human rationality level on learning rewards from multiple feedback

- types. In *Proceedings of the Thirty-Seventh AAAI Conference on Artificial Intelligence and Thirty-Fifth Conference on Innovative Applications of Artificial Intelligence and Thirteenth Symposium on Educational Advances in Artificial Intelligence*, AAAI’23/IAAI’23/EAAI’23. AAAI Press, 2023. ISBN 978-1-57735-880-0. doi: 10.1609/aaai.v37i5.25740. URL <https://doi.org/10.1609/aaai.v37i5.25740>.
- [43] Lauren Milliken and Geoffrey A. Hollinger. Modeling user expertise for choosing levels of shared autonomy. In *2017 IEEE International Conference on Robotics and Automation (ICRA)*, pages 2285–2291, 2017. doi: 10.1109/ICRA.2017.7989263.
- [44] Juho Lee, Yoonho Lee, Jungtaek Kim, Adam Kosior, Seungjin Choi, and Yee Whye Teh. Set transformer: A framework for attention-based permutation-invariant neural networks. In Kamalika Chaudhuri and Ruslan Salakhutdinov, editors, *Proceedings of the 36th International Conference on Machine Learning*, volume 97 of *Proceedings of Machine Learning Research*, pages 3744–3753. PMLR, 09–15 Jun 2019. URL <https://proceedings.mlr.press/v97/lee19d.html>.
- [45] Ashish Vaswani, Noam Shazeer, Niki Parmar, Jakob Uszkoreit, Llion Jones, Aidan N Gomez, Łukasz Kaiser, and Illia Polosukhin. Attention is all you need. In I. Guyon, U. Von Luxburg, S. Bengio, H. Wallach, R. Fergus, S. Vishwanathan, and R. Garnett, editors, *Advances in Neural Information Processing Systems*, volume 30. Curran Associates, Inc., 2017.
- [46] Yuchen Cui, Qiping Zhang, W. Bradley Knox, Alessandro Allievi, Peter Stone, and Scott Niekum. The EMPATHIC framework for task learning from implicit human feedback. In Jens Kober, Fabio Ramos, and Claire J. Tomlin, editors, *4th Conference on Robot Learning, CoRL 2020, 16-18 November 2020, Virtual Event / Cambridge, MA, USA*, volume 155 of *Proceedings of Machine Learning Research*, pages 604–626. PMLR, 2020. URL <https://proceedings.mlr.press/v155/cui21a.html>.
- [47] Tianhe Yu, Deirdre Quillen, Zhanpeng He, Ryan Julian, Karol Hausman, Chelsea Finn, and Sergey Levine. Meta-world: A benchmark and evaluation for multi-task and meta reinforcement learning. In Leslie Pack Kaelbling, Danica Kragic, and Komei Sugiyama, editors, *3rd Annual Conference on Robot Learning, CoRL 2019, Osaka, Japan, October 30 - November 1, 2019, Proceedings*, volume 100 of *Proceedings of Machine Learning Research*, pages 1094–1100. PMLR, 2019. URL <http://proceedings.mlr.press/v100/yu20a.html>.
- [48] Arsenii Kuznetsov, Pavel Shvechikov, Alexander Grishin, and Dmitry Vetrov. Controlling overestimation bias with truncated mixture of continuous distributional quantile critics. In Hal Daumé III and Aarti Singh, editors, *Proceedings of the 37th International Conference on Machine Learning*, volume 119 of *Proceedings of Machine Learning Research*, pages 5556–5566. PMLR, 13–18 Jul 2020. URL <https://proceedings.mlr.press/v119/kuznetsov20a.html>.
- [49] John Schulman, Filip Wolski, Prafulla Dhariwal, Alec Radford, and Oleg Klimov. Proximal policy optimization algorithms, 2017. URL <https://arxiv.org/abs/1707.06347>.
- [50] Antonin Raffin, Ashley Hill, Adam Gleave, Anssi Kanervisto, Maximilian Ernestus, and Noah Dormann. Stable-baselines3: Reliable reinforcement learning implementations. *Journal of Machine Learning Research*, 22(268):1–8, 2021. URL <http://jmlr.org/papers/v22/20-1364.html>.
- [51] Adam Gleave, Mohammad Tafaeque, Juan Rocamonde, Erik Jenner, Steven H. Wang, Sam Toyer, Maximilian Ernestus, Nora Belrose, Scott Emmons, and Stuart Russell. imitation: Clean imitation learning implementations. arXiv:2211.11972v1 [cs.LG], 2022. URL <https://arxiv.org/abs/2211.11972>.
- [52] Jonathan Ho and Stefano Ermon. Generative adversarial imitation learning. In D. Lee, M. Sugiyama, U. Luxburg, I. Guyon, and R. Garnett, editors, *Advances in Neural Information Processing Systems*, volume 29. Curran Associates, Inc., 2016.
- [53] Justin Fu, Katie Luo, and Sergey Levine. Learning robust rewards with adversarial inverse reinforcement learning. In *International Conference on Learning Representations*, 2018. URL <https://openreview.net/forum?id=rkHyw1-A->.
- [54] Paul F Christiano, Jan Leike, Tom Brown, Miljan Martic, Shane Legg, and Dario Amodei. Deep reinforcement learning from human preferences. In I. Guyon, U. Von Luxburg, S. Bengio, H. Wallach, R. Fergus, S. Vishwanathan, and R. Garnett, editors, *Advances in Neural Information Processing Systems*, volume 30. Curran Associates, Inc., 2017.
- [55] Maxime Oquab, Timothée Darcet, Théo Moutakanni, Huy V. Vo, Marc Szafraniec, Vasil Khalidov, Pierre Fernandez, Daniel HAZIZA, Francisco Massa, Alaaeldin El-Nouby, Mido Assran, Nicolas Ballas, Wojciech Galuba, Russell Howes, Po-Yao Huang, Shang-Wen Li, Ishan Misra, Michael Rabbat, Vasu Sharma, Gabriel Synnaeve, Hu Xu, Herve Jegou, Julien Mairal, Patrick Labatut, Armand Joulin, and Piotr Bojanowski. DINOv2: Learning robust visual features without supervision. *Transactions on Machine Learning Research*, 2024. ISSN 2835-8856. URL <https://openreview.net/forum?id=a68SUt6zFt>. Featured Certification.

- [56] Matteo Pirota, Andrea Tirinzoni, Ahmed Touati, Alessandro Lazaric, and Yann Ollivier. Fast imitation via behavior foundation models. In *The Twelfth International Conference on Learning Representations*, 2024. URL <https://openreview.net/forum?id=qnWtw310jb>.
- [57] Tom Brown, Benjamin Mann, Nick Ryder, Melanie Subbiah, Jared D Kaplan, Prafulla Dhariwal, Arvind Neelakantan, Pranav Shyam, Girish Sastry, Amanda Askell, Sandhini Agarwal, Ariel Herbert-Voss, Gretchen Krueger, Tom Henighan, Rewon Child, Aditya Ramesh, Daniel Ziegler, Jeffrey Wu, Clemens Winter, Chris Hesse, Mark Chen, Eric Sigler, Mateusz Litwin, Scott Gray, Benjamin Chess, Jack Clark, Christopher Berner, Sam McCandlish, Alec Radford, Ilya Sutskever, and Dario Amodei. Language models are few-shot learners. In H. Larochelle, M. Ranzato, R. Hadsell, M.F. Balcan, and H. Lin, editors, *Advances in Neural Information Processing Systems*, volume 33, pages 1877–1901. Curran Associates, Inc., 2020.
- [58] Bodhisattva Sen. A gentle introduction to empirical process theory and applications, July 2022. <http://www.stat.columbia.edu/~bodhi/Talks/Emp-Proc-Lecture-Notes.pdf>.
- [59] Diederik P. Kingma and Jimmy Ba. Adam: A method for stochastic optimization. In Yoshua Bengio and Yann LeCun, editors, *3rd International Conference on Learning Representations, ICLR 2015, San Diego, CA, USA, May 7-9, 2015, Conference Track Proceedings*, 2015. URL <http://arxiv.org/abs/1412.6980>.

A Proof of the Bayes Optimality of SRI

In this section, we use the Bayesian inverse reinforcement learning framework [6] to show that any “ideal” SRI algorithm is asymptotically optimal for both reward inference and imitation learning (see Theorem A.4 for details). In particular, our analysis relies on only three main assumptions for the SRI algorithm and the problem: niceness and compactness of the function class and MDP, appropriate model capacity, and data coverage.

Our proof proceeds as follows: first, in Section A.1, we lay out our notation and assumptions; second, in Section A.2, we derive the closed form of the Bayes-optimal reward function for imitation given limited behavior trajectories; third, in Section A.3, we show that SRI converges uniformly in the limit of infinite data to this Bayes-optimal reward function; finally, in Section A.4, we use these results to prove that the optimal policies for SRI also converge uniformly to Bayes optimality, i.e., they asymptotically provide the maximum possible expected return given irreducible uncertainty about the ground truth reward function.

A.1 Preliminaries

Notation: Each of the sets we consider generally has at most one σ -algebra associated with it. Thus, as standard in probability theory, we will often use each set interchangeably with its measurable space.

Let \mathcal{R} be a measurable space of reward functions in \mathcal{M} , equipped with any σ -algebra, and let $\mathcal{P}(\mathcal{R})$ be the set of all probability measures with respect to \mathcal{R} ’s σ -algebra. (Define the operator \mathcal{P} similarly for any measurable space.) Let $P \in \mathcal{P}(\mathcal{R})$ be the ground-truth marginal distribution of reward functions; in particular, these reward functions are potentially co-dependent with behavior trajectories of maximum length L_B . For any number of trajectories N define the task-generating distribution

$$\mathcal{D}_R \in \mathcal{P}(\mathcal{R} \times \mathcal{T}^N).$$

Rather than seeing the actual reward function, an SRI algorithm sees a set of M state-reward pairs. In particular, let $P_S \in \mathcal{P}(\mathcal{S})$ be a distribution over states. The data-generating distribution is defined by the following process: first, for dataset size (number of tasks) K , take K i.i.d. samples

$$\{(R_k, \{\tau_{k,n}\}_{n=1}^N)\}_{k=1}^K$$

from \mathcal{D}_R , then sample M states from P_S for each task:

$$\{s_{k,m}\}_{k=1, m=1}^{K, M}.$$

Finally, label each state $s_{k,m}$ with its reward for SRI to predict, $R_k(s_{k,m})$. The resulting dataset has K tasks, and each task has N trajectories and M state-reward pairs:

$$\left\{ \left(\{(s_{k,m}, R_k(s_{k,m}))\}_{m=1}^M, \{\tau_{k,n}\}_{n=1}^N \right) \right\}_{k=1}^K.$$

We aim to learn a parameterized reward function $R_\theta : \mathcal{S} \times \mathcal{T}^N \rightarrow \mathbb{R}$ on this dataset, for θ in some space Θ (see Assumption 1).

Notation For brevity, we henceforth omit index specifications when they are clear from context; e.g., $\{\tau_n\} := \{\tau_n\}_{n=1}^N$, and similar for sequences. Furthermore, in conditional statements we omit the conditioned random variable when it is clear from context: $\mathbb{E}[Y|x] := \mathbb{E}[Y|X = x]$.

We first lay out all assumptions necessary for our results.

Assumption 1 (Well-Behaved Spaces and Functions). **(a)** The state space \mathcal{S} , observation space \mathcal{O} , and action space \mathcal{A} are compact measurable metric spaces equipped with σ -algebras $\mathcal{F}_\mathcal{S}$, $\mathcal{F}_\mathcal{O}$ and $\mathcal{F}_\mathcal{A}$, respectively, and all relevant probability measures (e.g., $\pi(s)$ for any $s \in \mathcal{S}$) are defined with respect to $\mathcal{F}_\mathcal{S}$, $\mathcal{F}_\mathcal{O}$, and $\mathcal{F}_\mathcal{A}$. (It follows that \mathcal{T}^N is also a compact metric space, using some reasonable product metric.) **(b)** The transition probability function $p : \mathcal{S} \times \mathcal{A} \rightarrow \mathcal{P}(\mathcal{A})$ is a Markov kernel (hence measurable), all policies $\pi : \mathcal{S} \rightarrow \mathcal{P}(\mathcal{A})$ is a Markov kernel, and the reward function $R : \mathcal{S} \rightarrow \mathbb{R}$ is measurable. **(c)** The space Θ of reward model parameters is compact. **(d)** $R_\theta(s, \{\tau_n\})$ is measurable and continuous with respect to θ , s , and $\{\tau_n\}$, and $\{R_\theta\}_{\theta \in \Theta}$ is equicontinuous in s and $\{\tau_n\}$. **(e)** All measure spaces are σ -finite.

Remark A.1. Compactness of Θ and \mathcal{S} and equicontinuity (Assumption 1(a, c, d)) imply that $\{R_\theta\}_{\theta \in \Theta}$ is uniformly bounded.

Assumption 2 (Bounded Returns). All reward functions $R \in \mathcal{R}$ are bounded, and either $\gamma < 1$ or $\exists L \in \mathbb{Z}_{\geq 0}$ such that for all $t > L$, $R_t = 0$. Therefore, all returns are bounded, and J_θ is bounded for all θ .

Assumption 3 (MSE). In this section, SRI is defined using squared error over the dataset. In particular, we define the single-sample loss for a parameter θ as

$$\ell_\theta(R, \{\tau_n\}, s) = (R_\theta(s, \{\tau_n\}) - R(s))^2.$$

Remark A.2. We do not assume the uniqueness of minimizing parameters, but our definitions naturally imply unique minimizing functions.

Assumption 4 (Model Capacity). The hypothesis class $\{R_\theta\}$ contains $\bar{R}_\dagger := \mathbb{E}[R \mid \{\tau_n\}]$, which Lemma A.3 shows to be the optimal reward function for maximizing expected imitation return.

Assumption 5 (Data Coverage). The data distribution over states has full support on \mathcal{S} : $\text{supp}(P_S) = \mathcal{S}$. (If the MDP contains unreachable states for any reason, the support need not include those states.)

A.2 Optimality of \bar{R} as a reward function for imitation

We first adapt a tabular result by Ramachandran and Amir [6] to show that, when optimizing expected return under an uncertain reward function, it is always optimal to optimize return under the expected value of that reward function.

Lemma A.3. Let $M_R = (\mathcal{S}, \mathcal{A}, p, R, d_0, \gamma)$ be an MDP with random reward function R following any distribution $P_R \in \mathcal{P}(\mathcal{R})$. Define the expected reward function $\bar{R} : \mathcal{S} \rightarrow \mathbb{R}$ to be $\bar{R}(s) = \mathbb{E}[R(s)]$. Then, the policy π^* that maximizes the expected cumulative reward $\mathbb{E}_R[J_R(\pi)]$, where

$$J_R(\pi) = \mathbb{E} \left[\sum_{t=0}^{\infty} \gamma^t R(S_t) ; \pi \right],$$

is an optimal policy for the MDP $M_{\bar{R}} = (\mathcal{S}, \mathcal{A}, p, \bar{R}, d_0, \gamma)$ with reward function \bar{R} . Similarly, any optimal policy for $M_{\bar{R}}$ is also optimal under J_R .

Proof. We aim to show that

$$\mathbb{E}[J_R(\pi)] = \mathbb{E} \left[\sum_{t=0}^{\infty} \gamma^t \bar{R}(S_t) ; \pi \right], \quad (1)$$

where the left expectation is taken over both the randomness in R and the stochastic transitions in the MDP under policy π , while the right expectation is taken over the latter alone.

The proof establishes the following equalities:

$$\mathbb{E}_R[J_R(\pi)] = \mathbb{E}_R \left[\mathbb{E} \left[\sum_{t=0}^{\infty} \gamma^t R(S_t) ; \pi \right] \right] \quad (2)$$

$$= \mathbb{E} \left[\mathbb{E}_R \left[\sum_{t=0}^{\infty} \gamma^t R(S_t) \right] ; \pi \right] \quad (3)$$

$$= \mathbb{E} \left[\sum_{t=0}^{\infty} \gamma^t \mathbb{E}_R[R(S_t)] ; \pi \right]. \quad (4)$$

Step (A.2) \rightarrow (A.2) follows immediately from Assumption 2 and the Bounded Convergence Theorem. Therefore, all that remains is to justify the application of Fubini's Theorem in step (A.2) \rightarrow (A.2).

Let $(\Omega, \mathcal{F}, \mu)$ be the product measure space of reward functions and trajectories, where $\Omega = \mathcal{R} \times \mathcal{S}^\infty$, $\mathcal{F} = \mathcal{R} \otimes \mathcal{S}^\infty$ (using the usual cylinder σ -algebra), and $\mu = P(R) \times \mathbb{P}_\pi$. Here, \mathbb{P}_π is the probability measure over trajectories induced by π in this MDP.

Define the function $f(R, \{S_t\}) = \sum_{t=0}^{\infty} \gamma^t R(S_t)$.

To apply Fubini's Theorem, we need to verify that f is measurable with respect to \mathcal{F} and that $\int_\Omega |f| d\mu < \infty$.

Measurability: First, note that the projection of Ω onto each individual S_t is measurable by definition of the cylinder σ -algebra; thus, because R is measurable by assumption, each summand of f is individually measurable. The function f is therefore the limit of finite sums of measurable functions, and hence is measurable.

Integrability: For some non-negative $c \in \mathbb{R}$, whose exact value depends on γ and L (if applicable) we have

$$\begin{aligned} \int_\Omega |f| d\mu &= \int_{\mathcal{R}} \int_{\mathcal{S}^\infty} \left| \sum_{t=0}^{\infty} \gamma^t R(S_t) \right| d\mathbb{P}_\pi(\{S_t\}) dP(R) \\ &= \mathbb{E}_{R, S_t} \left[\left| \sum_{t=0}^{\infty} \gamma^t R(S_t) \right| \right] \\ &\leq \mathbb{E}_{R, S_t} [c], \end{aligned}$$

by Assumption 2.

Thus, we have established (A.2). To conclude, since the expected cumulative reward under the distribution $P(R)$ equals the expected cumulative reward in the MDP with reward function \bar{R} , maximizing $\mathbb{E}[J_R(\pi)]$ over policies π is equivalent to maximizing $J_{\bar{R}}(\pi)$ in the MDP $M' = (\mathcal{S}, \mathcal{A}, p, \gamma, \bar{R})$.

Therefore, the policy π^* that maximizes $\mathbb{E}[J_R(\pi)]$ is the optimal policy for the MDP with reward function \bar{R} . \square

Equipped with the result of Lemma A.3, we now show that, under our assumptions, any SRI algorithm asymptotically produces optimal policies for \bar{R} , and thus optimal policies for the posterior distribution over rewards, $P_R|_{\{\tau_n\}}$.

A.3 Convergence of (R_{θ_K})

The first step is to demonstrate the convergence of the learned SRI model in the limit of infinite data. First, we define our

risk functions in a manner that allows us to invoke a Glivenko-Cantelli argument [58]. As discussed in the preliminaries, consider a single sample $(R, \{\tau_n\}, s)$ drawn according to $\mathcal{D}_R \times P_S$, where $(R, \{\tau_n\}) \sim \mathcal{D}_R$ and $s \sim P_S$. The population risk is then

$$L(\theta) = \mathbb{E}_{(R, \{\tau_n\}) \sim \mathcal{D}_R, s \sim P_S} [\ell_\theta(R, \{\tau_n\}, s)].$$

Remark A.4. As always for least squares problems, for any

$$\theta^* \in \arg \min_{\theta \in \Theta} L(\theta),$$

we know $R_{\theta^*} = \bar{R}_l$.

Remark A.4 and Lemma A.3 show that the optimal reward function for MSE SRI indeed produces Bayesian-optimal policies. We must now show that this happens in the limit of infinite data, as well. Specifically, we show: 1) that SRI algorithms indeed converge to some optimal θ^* ; 2) that this convergence is uniform in the state space; 3) that uniform convergence implies convergence of the optimal policies. Steps 1 and 2 follow from standard learning theory patterns in Lemmas A.7 and A.8. Step 3 is completed in Theorem A.4.

Given a dataset of K tasks and M state samples per task,

$$\{(R_k, \{\tau_{n,k}\})\}_{k=1}^K \sim \mathcal{D}_R^K, \quad \{s_{m,k}\}_{m=1}^M \sim P_S^M,$$

we form the empirical risk:

$$\hat{L}_K(\theta) = \frac{1}{KM} \sum_{k=1}^K \sum_{m=1}^M \ell_\theta(R_k, \{\tau_{n,k}\}, s_{m,k}).$$

Remark A.5. Under Assumptions 1, 2, and 3, l_θ , $L(\theta)$ and $\hat{L}_K(\theta)$ are all bounded, continuous and measurable. (See Remark A.1.)

Remark A.6. Because increasing K provides additional data of all types, we can ignore M in the empirical risk (M need not approach ∞). In particular, note that $L(\theta)$ remains the same even if l_θ is a sample risk over states s_m (i.e., a loss for all state-reward samples in a single task) instead of a loss for one individual sample.

We can now show both pointwise and uniform convergence of R_{θ_K} .

Lemma A.7 (Pointwise Convergence of R_{θ_K}). *Suppose $\theta_K \in \arg \min_{\theta \in \Theta} \hat{L}_K(\theta)$ for each K . Under Assumptions 1–5, even without a unique minimizer θ^* , we have for all $(s, \{\tau_n\})$:*

$$R_{\theta_K}(s, \{\tau_n\}) \xrightarrow{a.s.} \bar{R}_l(s, \{\tau_n\}).$$

Proof. As usual for this type of result, our proof follows three steps: **1)** we show that l_θ is Glivenko-Cantelli; **2)** we conclude that \hat{L}_K almost surely converges uniformly to L ; **3)** we use the existence of a convergent subsequence θ_{K_j} to conclude the desired result.

Steps 1 and 2 By Remark A.5, we can directly conclude that l_θ is Glivenko-Cantelli [see, for example, Remark 3.1 and Theorem 3.2, 58]. Thus, by definition, \hat{L}_K almost surely uniformly converges to L :

$$\sup_{\theta \in \Theta} |\hat{L}_K(\theta) - L(\theta)| \xrightarrow{a.s.} 0.$$

Step 3 Because Θ is compact, and because all minimizers of $L(\theta)$ produce the same function (see Remark A.4), it is nearly sufficient to show that any convergent subsequence of θ_K converges to a minimizer of $L(\theta)$.

Since Θ is compact, let (θ_{K_j}) be a convergent subsequence of θ_K , and let θ^* be its limit. Fix $\varepsilon > 0$, and set K_0 such that for all $K' \geq K_0$, $\sup_{\theta \in \Theta} |\hat{L}_{K'}(\theta) - L(\theta)| < \frac{\varepsilon}{2}$. Set j' such that 1) $K_{j'} \geq K_0$, and 2) $|L(\theta_{K_{j'}}) - L(\theta^*)| < \frac{\varepsilon}{2}$ (recall that L is continuous). Then

$$\begin{aligned} |L_{K_{j'}}(\theta_{K_{j'}}) - L(\theta^*)| &\leq |L_{K_{j'}}(\theta_{K_{j'}}) - L(\theta_{K_{j'}})| \\ &\quad + |L(\theta_{K_{j'}}) - L(\theta^*)| \\ &< \frac{\varepsilon}{2} + \frac{\varepsilon}{2} \\ &= \varepsilon, \end{aligned}$$

so $L_{K_{j'}}(\theta_{K_{j'}}) \xrightarrow{a.s.} L(\theta^*)$. But by definition, for any $\theta \in \Theta$,

$$\begin{aligned} L_{K_{j'}}(\theta_{K_{j'}}) &\leq L_{K_{j'}}(\theta) \\ \Rightarrow \lim_{j \rightarrow \infty} L_{K_{j'}}(\theta_{K_{j'}}) &\leq \lim_{j \rightarrow \infty} L_{K_{j'}}(\theta) \\ \Rightarrow L(\theta^*) &\leq L(\theta). \end{aligned}$$

Hence, $\theta^* \in \arg \min_{\theta' \in \Theta} L(\theta')$. Letting $\Theta \supseteq \Theta^* = \arg \min_{\theta \in \Theta} L(\theta)$, we therefore conclude by compactness of Θ that $d(\theta_K, \Theta^*) \xrightarrow{a.s.} 0$. The desired result follows by continuity of R_θ . \square

Lemma A.8 (Uniform Convergence of (R_{θ_K})). *Define θ_K as in Lemma A.7. Given the equicontinuity of $\{R_\theta\}$, we also have almost sure uniform convergence of (R_{θ_K}) across $(s, \{\tau_n\})$:*

$$\|R_{\theta_K} - \bar{R}_l\|_\infty \xrightarrow{a.s.} 0.$$

Proof. The desired result follows smoothly from pointwise convergence and the Arzelà-Ascoli Theorem.

If (R_{θ_K}) did not converge uniformly to $\bar{R}_l(s) = \mathbb{E}[R(s)|\{\tau_n\}]$, then there would exist an $\varepsilon > 0$, a subsequence $(R_{\theta_{K_i}})$, and a sequence $((s_i, \{\tau_n\}_i))$ such that

$$|R_{\theta_{K_i}}(s_i, \{\tau_n\}_i) - \bar{R}_l(s_i, \{\tau_n\}_i)| \geq \varepsilon \text{ for all } i.$$

Of course, this subsequence also satisfies the conditions of Arzelà-Ascoli – most notably, equicontinuity – so we can extract a further uniformly convergent subsequence $(R_{\theta_{K_{ij}}})$. By Lemma A.7, we know that pointwise, $(R_{\theta_{K_{ij}}})$ almost surely converges to \bar{R}_l (using the same event for almost sure convergence as all other almost sure convergences here).

But this contradicts the assumption that $|R_{\theta_{K_i}}(s_i, \{\tau_n\}_i) - \bar{R}_l(s_i, \{\tau_n\}_i)| \geq \varepsilon$. Thus, (R_{θ_K}) must converge uniformly. \square

⁴Standard point-set distance: $d(x, A) = \inf_{a \in A} |x - a|$.

A.4 Convergence of SRI's optimal policies to Bayesian optimality

Finally, we conclude that any SRI algorithm satisfying our assumptions produces asymptotically Bayes-optimal policies.

Main Theorem (Asymptotic Optimality of SRI Algorithms). *Let $\mathcal{M}_R = (\mathcal{S}, \mathcal{A}, p, R, d_0, \gamma)$ be an MDP with random reward R , which is drawn together with $\{\tau_n\}$ from a distribution $\mathcal{D}_R \in \mathcal{P}(\mathcal{R} \times \mathcal{T}^N)$.*

Claim: *Any SRI algorithm satisfying Assumptions 1–5 is asymptotically optimal in the sense that the policies it produces approach those that maximize the expected return under the posterior distribution of R given $\{\tau_n\}$.*

Uniform Convergence of Inferred Rewards By Lemma A.8, we have that as $K \rightarrow \infty$,

$$\|R_{\theta_K} - \bar{R}_l\|_\infty \xrightarrow{\text{a.s.}} 0.$$

Here \bar{R}_l is the Bayesian-optimal reward function, as shown in Lemma A.3. In particular, \bar{R}_l is the reward function that, if known, would yield the policy maximizing the expected return given $\{\tau_n\}$.

Thus, for any $\delta > 0$, there exists K_δ such that for all $K > K_\delta$,

$$\|R_{\theta_K} - \bar{R}_l\|_\infty < \delta.$$

Policy Convergence Let $\pi_{\theta_K}^*$ be any optimal policy for the MDP $(\mathcal{S}, \mathcal{A}, p, R_{\theta_K}, d_0, \gamma)$. We wish to show that $\{\pi_{\theta_K}^*\}$ approaches optimality for \bar{R}_l as $K \rightarrow \infty$.

Define the value functions under a reward function R' and policy π as:

$$V_{R'}^\pi(s) = \mathbb{E} \left[\sum_{t=0}^{\infty} \gamma^t R'(S_t) \mid S_0 = s, \pi \right].$$

Let $V_{R_{\theta_K}}^*(s) = V_{R_{\theta_K}}^{\pi_{\theta_K}^*}(s)$ be the optimal value under R_{θ_K} , and let $V_{\bar{R}_l}^*(s)$ be the optimal value under \bar{R}_l .

We know:

$$V_{R_{\theta_K}}^{\pi_{\theta_K}^*}(s) \geq V_{R_{\theta_K}}^\pi(s), \quad \forall \pi.$$

We want to relate $V_{\bar{R}_l}^{\pi_{\theta_K}^*}$ to $V_{\bar{R}_l}^*$. Consider the difference:

$$V_{\bar{R}_l}^*(s) - V_{\bar{R}_l}^{\pi_{\theta_K}^*}(s).$$

Introduce the intermediate value functions under R_{θ_K} :

$$\begin{aligned} V_{\bar{R}_l}^*(s) - V_{\bar{R}_l}^{\pi_{\theta_K}^*}(s) &= [V_{\bar{R}_l}^*(s) - V_{R_{\theta_K}}^*(s)] \\ &\quad + [V_{R_{\theta_K}}^*(s) - V_{\bar{R}_l}^{\pi_{\theta_K}^*}(s)]. \end{aligned}$$

We will bound each piece.

Bounding $|V_{\bar{R}_l}^*(s) - V_{R_{\theta_K}}^*(s)|$: Because $\|R_{\theta_K} - \bar{R}_l\|_\infty < \delta$, we have for any policy π :

$$\begin{aligned} |V_{R_{\theta_K}}^\pi(s) - V_{\bar{R}_l}^\pi(s)| &\leq \mathbb{E} \left[\sum_{t=0}^{\infty} \gamma^t |R_{\theta_K}(S_t) - \bar{R}_l(S_t)| \right] \\ &\leq \frac{\delta}{1-\gamma}. \end{aligned}$$

Thus:

$$\|V_{R_{\theta_K}}^\pi - V_{\bar{R}_l}^\pi\|_\infty \leq \frac{\delta}{1-\gamma}, \quad \text{for any } \pi.$$

In particular, this applies to the optimal policies under either reward:

$$|V_{\bar{R}_l}^*(s) - V_{R_{\theta_K}}^*(s)| \leq \frac{\delta}{1-\gamma}.$$

Bounding $|V_{R_{\theta_K}}^*(s) - V_{\bar{R}_l}^{\pi_{\theta_K}^*}(s)|$: By optimality of $\pi_{\theta_K}^*$ under R_{θ_K} ,

$$V_{R_{\theta_K}}^*(s) = V_{R_{\theta_K}}^{\pi_{\theta_K}^*}(s).$$

Thus:

$$V_{R_{\theta_K}}^*(s) - V_{\bar{R}_l}^{\pi_{\theta_K}^*}(s) = [V_{R_{\theta_K}}^{\pi_{\theta_K}^*}(s) - V_{\bar{R}_l}^{\pi_{\theta_K}^*}(s)].$$

This difference is bounded by the same $\frac{\delta}{1-\gamma}$ argument as above:

$$|V_{R_{\theta_K}}^{\pi_{\theta_K}^*}(s) - V_{\bar{R}_l}^{\pi_{\theta_K}^*}(s)| \leq \frac{\delta}{1-\gamma}.$$

Combining these results, we have:

$$V_{\bar{R}_l}^*(s) - V_{\bar{R}_l}^{\pi_{\theta_K}^*}(s) \leq \frac{\delta}{1-\gamma} + \frac{\delta}{1-\gamma} = \frac{2\delta}{1-\gamma}.$$

Since $\delta > 0$ was arbitrary and can be made as small as desired by taking K sufficiently large, for any $\varepsilon > 0$, choose $\delta = \frac{\varepsilon(1-\gamma)}{2}$. Then for all $K > K_\delta$,

$$V_{\bar{R}_l}^*(s) - V_{\bar{R}_l}^{\pi_{\theta_K}^*}(s) \leq \varepsilon.$$

Therefore:

$$V_{\bar{R}_l}^{\pi_{\theta_K}^*}(s) \geq V_{\bar{R}_l}^*(s) - \varepsilon, \quad \forall s \in \mathcal{S},$$

and in particular

$$J_{\bar{R}_l}(\pi_{\theta_K}^*) \geq J_{\bar{R}_l}^* - \varepsilon.$$

Conclusion We have shown that as $K \rightarrow \infty$, the SRI algorithm's inferred reward functions R_{θ_K} converge uniformly to \bar{R}_l , and that the corresponding optimal policies $\pi_{\theta_K}^*$ approach optimality under \bar{R}_l . Since \bar{R}_l the Bayesian-optimal reward given $\{\tau_n\}$ (Lemma A.3), the policies derived from the SRI algorithm asymptotically maximize the expected return under the posterior over R .

B Architecture Details

We encoded trajectories using a 3-head transformer with two 256-dimensional transformer layers and a final 2-layer MLP with hidden dimension 50, outputting a trajectory representation of length 100; processed trajectory encodings into a task encoding with a default set transformer [44] with hidden dimension 128, outputting a task representation of dimension 256; encoded states using a 2-layer MLPs with hidden dimension 256 and encoding dimension 100; and processed task and state representations into a final reward with a 2-layer MLP of hidden dimension 256. All activations were leaky ReLU.

C Experimental Details

C.1 Tasks

Goals were selected randomly with $x \in [-0.3, 0.3]$, $y \in [0.4, 0.7]$, and $z \in [0.05, 0.3]$. For pick-place tasks, the object is randomly initialized per-episode for $x \in [-0.1, 0.1]$, $y \in [0.6, 0.7]$, and goals are chosen sufficiently far away to avoid initial success due to random object placement. All tasks used a horizon of 500. The default shaped reward functions were used both for SRI reward samples and ground-truth RL, except for the extra 5.0 success reward.

Note that the Meta-World reward is not computable from the default state representation; therefore, we provided SRI’s state encoder with augmented states during both training and RL. Specifically, we provided SRI with: the location and starting location of the left and right pads of the hand; the location of the “TCP (Tool Center Point) Center”; and the initial positions of the hand and the object. All of these values are computable from the history, but our goal in these experiments was not to test SRI’s performance in partially observable environments. Note that the learned policy did not see these augmented state dimensions.

Unfortunately, we could not augment states for the baseline algorithms to include initial position information, as doing so provided the adversarial discriminators with a “hack” to distinguish demonstrations from generated behavior, but we provided them with the TCP center and pad locations.

To simplify both supervised learning and reinforcement learning, we shifted and scaled all rewards to have the range $[-3, 3]$ (after adding the extra success reward of 5.0).

C.2 Demonstration Details

PSYCHIC_α details: Given goal position g and x-y origin $o_{x,y} = (0, 0.55)$, the hand reaches deterministically from its starting position towards target $t_{x,y} = o_{x,y} + \alpha(g_{x,y} - o_{x,y})$.

HARD details: the hand starts in a random position, then over 250 timesteps draws a 0.1-radius circle around the location of the goal mirrored through the x-y-z origin $o = (0, 0.55, 0.175)$. Note that the hand cannot always reach the far point of this circle, so the mirrored goal cannot be determined through averaging alone.

For GESTURE tasks, the hand starts in a random position satisfying $x \in [-0.4, 0.4]$, $y \in [0.4, 0.8]$, $z \in [0.1, 0.4]$.

C.3 SRI Training Details

SRI was trained for 2,000 epochs on all tasks with a batch size of 16 and learning rate of 0.0003, using the Adam optimizer [59].

As mentioned in Section 6.2, we found hacking of SRI’s rewards to be a particular problem in pick-place tasks, where a lack of model capacity forced SRI to trade off modeling the success reward on one hand and the grasping and pre-grasping shaped rewards on the other. SRI generally chose to optimize the success reward, as doing so was optimal for minimizing MSE, but this caused pick-place policies trained with the resulting reward to often fail to grasp the object at all. In order to encourage SRI to focus on modeling the non-success rewards, we linearly increased the proportion of pick-place state samples in the state-reward dataset from 5% to 20% over the course of training the reward model. However, the total proportion of reach and pick-place state samples per task was still 0.8 and 0.2, respectively; when necessary, we therefore sampled reach states with replacement to achieve the required total number of states per task.

C.4 Reinforcement Learning

The reason we used PPO for pick-place tasks and TQC for reach tasks is empirical: we found that PPO learned slowly in reach tasks and that TQC often failed to learn in pick-place tasks. All RL and baseline policies were trained for 5,000,000 environment interactions for reach tasks and 10,000,000 for pick-place tasks.

All networks of all RL policies were two-layer, hidden dimension 512 MLPs. For baselines, the actor had this structure, but the critic had the same structure as SRI’s state encoder: a two-layer MLP with hidden dimension 256.

All algorithms, RL and baseline, learned for 10,000,000 total environment interactions for pick-place tasks and 5,000,000 interactions for reach tasks. Baseline hyperparameters were set to equal RL hyperparameters where appropriate (e.g., number of interactions and network size), and otherwise were taken from their respective papers as much as possible. Behavioral cloning was trained for 50 epochs.

RL algorithms used batch sizes of 128, learning rates of 0.0001, and $\gamma = 0.9$. TQC used two critics, a rollout buffer size of 10,000,000, one update per transition, and a soft update coefficient of 0.005; PPO collected $2,048 \times 16$ transitions between updates and trained for 10 epochs per transition batch.

Note that the strangely poor behavior of the baselines in some conditions, such as AIRL in single-demonstration tasks and GAIL in noisy tasks, may in part be due to Meta-World tasks violating their assumptions. For example, GAIL assumes infinite-horizon tasks [52]. Nevertheless, as dominant imitation learning algorithms, we still believe them to be important baselines for comparison.